International Journal of Engineering Trends and Technology
ISSN: 2231–5381 / https://doi.org/10.14445/22315381/IJETT-V71I11P208

Volume 71 Issue 11, 84-89, November 2023

Original Article

Modelling and Analysis of ZnO Piezoelectric-Based Circular Diaphragm Pressure Sensor

Moirangthem Shamjit Singh[1*], Pradip Kumar Kalita[1], Heisnam Shanjit Singh[1], Maibam Sanju Meetei[2]

[1]*Department of Physics, Rajiv Gandhi University, Arunachal Pradesh, India.*
[2]*Department of Electronics and Communication Engineering, Rajiv Gandhi University, Arunachal Pradesh, India.*

[*]*Corresponding Author : shamjitmoirang@gmail.com*

Received: 10 July 2023 Revised: 21 September 2023 Accepted: 27 September 2023 Published: 04 November 2023

Abstract *- This paper illustrates the mathematical model and simulation of a ZnO piezoelectric-based circular diaphragm pressure sensor. The load stress analytical model and stress-voltage model of the sensor are described in the mathematical model in this study. The various parameters influencing the sensor's developed stress and output voltage are discussed. Among the various piezoelectric materials, namely PZT, PVDF, PMN-PT, $LiNbO_3$, AlN, and ZnO used for designing piezoelectric-based sensors, ZnO is adopted in this study as it has a high piezoelectric voltage coefficient with a value of $-4.85x10^{-2}$ Vm/N. For the purpose of validating the analytical model, simulations of the 3D model sensor are performed using the COMSOL Multiphysics Simulator. The output characteristics of the sensor are found linearly with applied pressure and with a negative slope during the validation of the analytical model using the simulated values. The negative charge is generated at the place where tensile stress is developed, and the positive charge is generated at the place where compressive stress is developed, as found in this work. It is shown that nearly equal sensitivities of the mathematical model and simulated model of the proposed sensors are respectively detected at -3.552 mV/kPa and -3.426 mV/kPa.*

Keywords *- Charge, Linear, Meshing, Sensitivity, Stress.*

1. Introduction

The need for extremely precise and effective sensors has become critical in today's technologically advanced society. One of the most adaptable and often utilised sensing technologies in various fields and applications is piezoelectric pressure sensors [1]. This piezoelectric pressure sensor has unique features that offer excellent sensitivity, accuracy, and durability by transforming induced stress into electrical quantity [2].

The basic working principle of the piezoelectric pressure sensor is that its internal structure changes when a piezoelectric material experiences mechanical pressure or stress, like compression or bending. A new distribution of charged particles occurs as a result of this deformation, creating an electric potential throughout the material.

This phenomenon of inducing electric potential on the deformation of materials due to mechanical pressure is called the direct piezoelectric effect. Contrarily, on the application of electric fields to a piezoelectric material, the charged particles within the material change their positions due to the mechanical deformation of the material. This phenomenon is known as the reverse piezoelectric effect. Thus, the piezoelectric effect is also a reversible process [3].

There are several sensor applications for piezoelectric materials, including energy harvesters, force, acceleration, pressure, vibration, and sound sensors. Because of their high linearity, high sensitivity, simplicity attached to other devices, flexibility and lightweight, this kind of pressure sensor have been the subject of extensive study and reporting.

The pressure sensor was created using a variety of different piezoelectric materials. Here are a few examples that are frequently used: Quartz, Lead Zirconate Titanate (PZT), Polyvinylidene Fluoride (PVDF), Lead Magnesium Niobate-Lead Titanate (PMN-PT), Lithium Niobate ($LiNbO_3$), Aluminium Nitride (AlN), and Zinc Oxide (ZnO) [4-6]. Among the different piezoelectric materials that are accessible, zinc oxide (ZnO) is regarded as one of the best. ZnO has also a very high piezoelectric voltage coefficient [7-9].

ZnO possesses a significant piezoelectric coupling coefficient, quantifying its capability to convert mechanical energy into electrical energy and vice versa. Excellent mechanical and electrical characteristics can be found in ZnO. ZnO is a versatile material that can be easily synthesised into a variety of shapes, such as thin films, bulk and nanowires. It has a high elastic modulus, meaning it can endure large stress and strain without deformation.

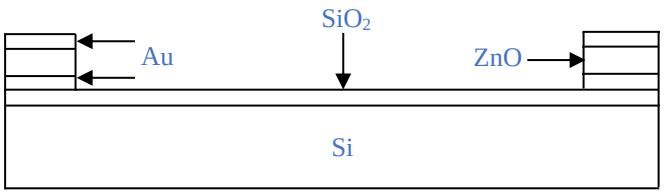

Fig. 1 Side-cut view of the circular-based pressure sensor

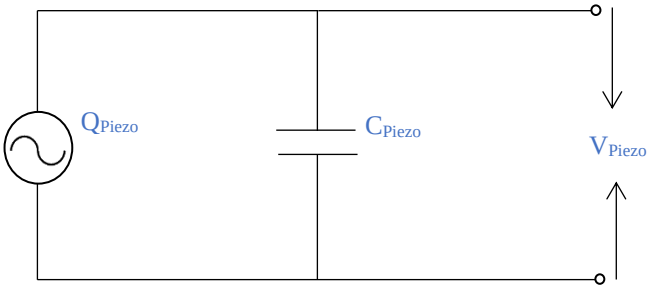

Fig. 2 Schematic diagram of a Piezoelectric sensor

ZnO piezoelectric pressure sensors can also be used in medical devices like blood pressure monitors, breathing equipment, infusion pumps, and catheters. Since they are made of a substance-free of lead or other heavy metals, they are applied in diagnosis, therapy, patient monitoring, and reliable measurement of physiological pressures.

The objectives of this study include developing a mathematical model for a diaphragm-based piezoelectric sensor characterized by exceptional linearity in its output across a pressure range of 0 kPa to 100 kPa, verifying the accuracy of the simulated output, and investigating the diverse parameters affecting the sensor's sensitivity.

2. Sensor Structure and its Equivalent Circuit

2.1. Sensor Structure

The fundamental design of the piezoelectric pressure sensor with a circular cross-section is shown in Fig. 1. ZnO is used as a piezoelectric sensing material in this investigation. The sensor substrate is silicon (Si), which serves as the main mechanical structure of the sensor.

The substrate body and electrode are separated from one another by a silicon dioxide (SiO_2) insulator. The top and base surfaces of the sensing layer are coated with gold (Au) and act as the sensor's electrodes to get the outputs.

2.2. Schematic Model

When a piezoelectric sensor deforms under the applied pressure, the piezoelectric sensing material is under stress as a result of the pressure or force being applied. Due to this deformation, Charges (Q_{Piezo}) are produced and accumulated on the opposite surface of the piezoelectric materials. The piezoelectric material's opposite sides experienced tensile stress and compressive stress, which caused the negative and positive charge to form between the two opposite surfaces and work as a capacitor (C_{Piezo}). These opposite charges created a potential difference (V_{Piezo}) between the top and base surfaces, which is the sensor's output. Its corresponding circuit diagram is shown in Fig. 2.

3. Analytical Model

This study uses the schematic model for a piezoelectric sensor to transform input pressure to output voltage. In order to convert, pressure is applied to the sensor's surface, which causes stress. As a result, output voltage is produced on the surface of the piezoelectric material. Therefore, it is essential to comprehend the sensor's load-stress model and stress-voltage model.

3.1. Load-Stress Model

Fig. 1 shows the fundamental structure of the circular diaphragm piezoelectric pressure sensor. The input pressure (P) is applied to the surface of the circular diaphragm. The circular diaphragm has a clamped edge at $r= a$ and for the center at $r = 0$. Because of the applied pressure, the deflection ($w(x,y)$) is produced on the diaphragm along with stress (T). The differential equation of a diaphragm can be solved to produce the desired deflection as done in [10-12]:

$$D\left(\frac{\partial^2}{\partial x^2}+\frac{\partial^2}{\partial y^2}\right)\left(\frac{\partial^2}{\partial x^2}+\frac{\partial^2}{\partial y^2}\right)w(x,y)=P, \qquad (1)$$

where D represents the flexure rigidity, which is given by:

$$D=\frac{Eh^3}{12(1-v^2)} \qquad (2)$$

Here, E denotes Young's modulus, v denotes the Poisson's ratio, and h is the thickness of the diaphragm.

The above equation 1 can be written in polar form as follows:

$$\frac{1}{r}\frac{d}{dr}\left(r\frac{d}{dr}\left(\frac{1}{r}\frac{d}{dr}\right)r\frac{d}{dr}w(r)\right)=\frac{P}{D} \qquad (3)$$

The above equation 3 is solved by applying the boundary conditions, i.e. deflection and derivatives of deflection at the edges ($r=a$) is zero, considering that there is no natural logarithm for zero. The equation 3 using equation 2 reduces to

$$w(r)=\frac{0.1875(1-v^2)P}{Eh^3}(a^2-r^2)^2 \qquad (4)$$

There are two types of stress based on the direction, namely- radial stress (T_r) and tangential stress (T_t). The mathematical expressions of T_r and T_t can be expressed by equation 5 and equation 6, respectively [10-12].

$$T_r=\frac{3a^2}{8h^2}P\left((3+v)\frac{r^2}{a^2}-(1+v)\right) \qquad (5)$$

$$T_t = \frac{3a^2}{8h^2} P \left((1+3v)\frac{r^2}{a^2} - (1+v) \right) \quad (6)$$

Now, the stress is estimated at different positions of the diaphragm. The T_r and T_t at the edges ($r=a$) and at the center ($r=0$) are obtained as:

$$T_r(a) = \frac{3a^2}{4h^2} P \quad (7)$$

$$T_t(a) = \frac{3a^2}{4h^2} Pv \quad (8)$$

$$T_r(0) = T_t(0) = -\frac{3a^2}{8h^2} P(1+v) \quad (9)$$

From the above equations 7, 8, and 9, it is obvious that the maximum stress has occurred at those edges in the radial direction as the values of Poisson's ratio are always less than one.

3.2. Stress-Voltage Model

A potential difference between the surfaces forms as charge accumulates on the opposite surface of the piezoelectric material, making it act as a capacitor. The electrical equivalent circuit is depicted in Fig. 2.

$$V = \frac{Q}{C}, \quad (10)$$

Where C represents the capacitance between the two piezoelectric surfaces, Q is the induced charges, and V is the output voltage.

It is a fact that the edges of the upper surface generate the highest tensile stress; this generated tensile stress is closely related to the generation of charges. Piezoelectric material is attached close to the diaphragm's edges to enable the generation of the highest possible output voltage.

The following is a description of the electrostatic charge that was created as a result of the generated stress on the surface of the sensing material [13-14]:

$$q(r) = d_{31} T_r(r) \quad (11)$$

Where $q(r)$ is the generated charge on the sensing material and d_{31} is the strain constant of the sensing material.

Now, let us consider a square-shaped piezoelectric material placed on the circular diaphragm. Let us consider l is the length of the square and the total charges developed on the surface of sensing material is Q, which is given by:

$$Q = d_{31} l^2 T_r(r) \quad (12)$$

Now, the capacitance of the square plates is given by:

$$C = \frac{\epsilon_{33} l^2}{t} \quad (13)$$

Where ε_{33} is the permittivity of the piezoelectric, and t is the thickness of the piezoelectric.

From above equation 12 and equation 13, the sensor output voltage V can be written as:

$$V = \frac{d_{31} t T_r(r)}{\epsilon_{33}} \quad (14)$$

The above equation 14 can be rewritten as:

$$V = g_{31} t T_r(r) \quad (15)$$

Where the value of g_{31} is given by

$$g_{31} = \frac{d_{31}}{\epsilon_{33}}. \quad (16)$$

The sensor's output voltage is closely related to factors like the piezoelectric material's thickness, surface-induced stress, and piezoelectric voltage coefficient.

3.3. Sensitivity

The ratio of the magnitude changes in the output signal to the magnitude changes in the input signal is known as the device's sensitivity. The sensitivity (S) is represented mathematically by:

$$S = \frac{V_x - V_y}{P_x - P_y}, \quad (17)$$

Where V_x and V_y are the output voltages corresponding to the applied pressure of P_x and P_y, respectively. The various parameter that influences the output voltages also influences the sensitivity.

4. Results and Discussion

The mathematical model is tested by fabricating the modelled sensor or by simulating the modelled sensor in a Finite Element Method simulator (FEM). FEM is frequently used to analyse quickly, clearly, and accurately depending on how various design parameters affect sensor performance. In this study, the sensor is simulated and constructed using COMSOL Multiphysics 5.2® to verify the accuracy of the mathematically derived sensor model.

4.1. Diaphragm Structure Design

From the Mathematical model, the radius of the diaphragm must be as wide as feasible, and the diaphragm thickness must be as tiny as feasible to achieve greater sensitivity [15]. Larger and thinner diaphragms, however, not only produce more nonlinearity but also more structural stress, which can lead to reliability problems. Given the aforementioned issues and the current process capacity, the diaphragm's side length should be less than 3500 μm, and its thickness should be greater than 20 μm.

In the COMSOL Multiphysics simulator, Fig. 3 depicts a 3D structure of the proposed sensor. The diaphragm radius of 150 μm and a thickness of 25 μm with Si material is used in this study, which is the most commonly used diaphragm dimension. On top of the silicon substrate, a SiO_2 insulator and its thickness of 5 (m) is placed

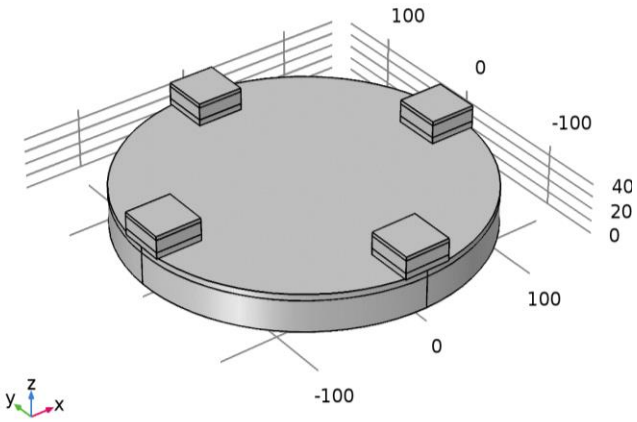

Fig. 3 The proposed 3D structure of the sensor in COMSOL

The thickness of the ZnO piezoelectric sensing material is 10 μm. The top and base of the sensing material are covered with 5 μm thick Gold (Au) electrodes. All the circumferences are fixed to form a circular diaphragm. The input pressures are applied on the top of the surface. The material properties utilized in the simulation are listed in the Table. 1

4.2. Initial and Boundary Condition

Before the simulation, selecting the appropriate Physics modules and setting the various initial conditions is crucial. This work uses solid mechanics, electrostatics, and piezoelectric modules as an interface between the two physics. First, the COMSOL model structure is established, and the relevant built-in materials are allocated to their respective components.

Following the completion of the physics setup, a finer tetrahedral meshing process is performed. After generating the mesh, the simulated sensor is examined and analysed within the simulator, covering a pressure range of 0 to 100 kPa in increments of 10 kPa.

4.3. Model Validation

Simulation analysis is done in COMSOL Multiphysics based on the proposed sensor model to verify the analytical model. The various parameters and dimensions are specified. Later, the simulation is run for the applied pressure range of 0-100 kPa, and various outputs are observed.

Table 1. Materials properties used in the simulation

Types of Material	Young's Modulus	Poisson's Ratio	Piezoelectric Voltage Coefficient
ZnO	120 GPa	0.36	-4.85×10^{-2} Vm/N
Au	70 GPa	0.44	-
SiO_2	70 GPa	0.17	-
Si	160 GPa	0.22	-

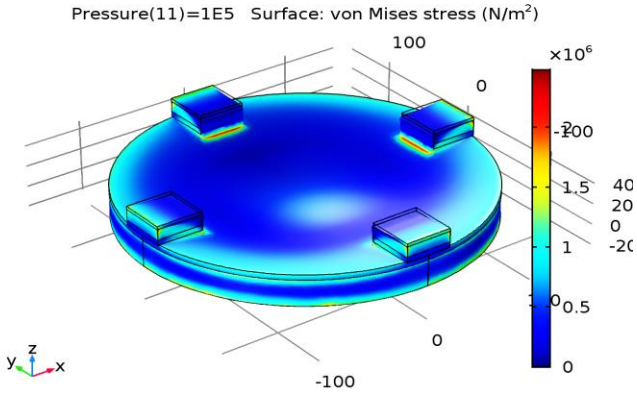

Fig. 4 Simulated output stress distribution on the sensor's surface with the 100 kPa

Fig. 4 depicts the stress distribution on the diaphragm surface for an applied pressure of 100 kPa on the sensor's surface. The sensor mathematical model shows that a symmetrical stress is created on the surface of a circular construction, and it also shows that the largest stress occurs at the edges of the sensor, which is also observed in the output of the stress distribution. It is also observed that the output stress is tensile stress on the surface.

Fig. 5 shows the simulated output voltage distribution on the sensing material at a 100 kPa applied pressure. In close proximity to the margins of the top layer of the sensor, the sensor displays a higher output voltage value. Additionally, it was noted that the upper surface of the piezoelectric material experienced a negative output voltage.

Fig. 6 depicts the output voltage of the sensor across a pressure range of 0 to 100 kPa for the simulation. Once again, the graph clearly illustrates that the voltage increases in magnitude when the applied pressure increases, but with negative values. This observation suggests a linear correlation between the pressure sensor's output and the applied pressure, characterized by a negative slope. The sensor's model equation further reflects this simulated output behavior.

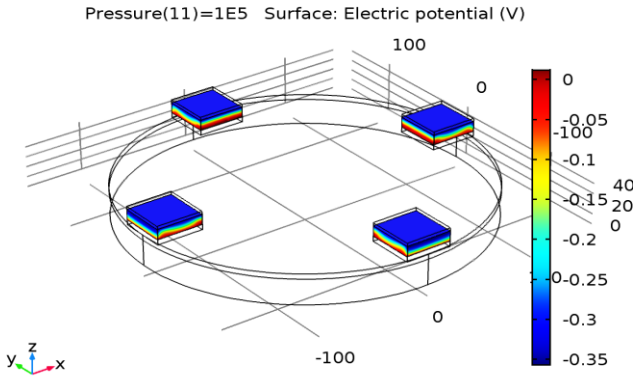

Fig. 5 Simulated output voltage distribution on the sensor surface applied by 100 kPa pressure

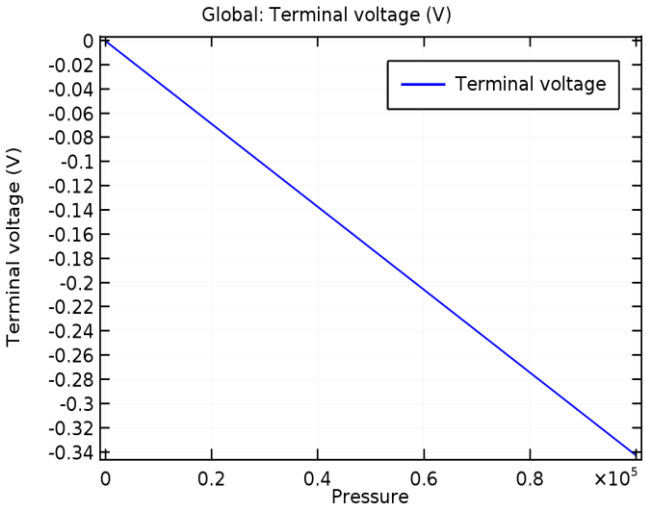

Fig. 6 Simulated output voltage graph of the sensor for the applied pressure range from 0 to 100 kPa

Table 2. Simulated and calculated values of voltage of the sensor

Applied Pressure [kPa]	Simulated Output Voltage [mV]	Analytical Output Voltage [mV]
0	0	0
10	-34.26	-35.52
20	-68.52	-71.0449
30	-102.79	-106.5674
40	-137.05	-142.0898
50	-171.31	-177.6123
60	-205.57	-213.1348
70	-239.84	-248.6572
80	-274.10	-284.1797
90	-308.36	-319.7021
100	-342.62	-355.2246

The proposed ZnO piezoelectric pressure-based circular diaphragm sensor for sensing pressure ranges from 0 to 100 kPa is shown in Table 2, along with the simulated and analytical output voltage values. The simulated output values and analytical values are seen to be relatively close to one another. Additionally, it has been noted that the magnitude of the estimated and simulated values increases with increasing applied pressure but with a negative slope. This research validates the suggested analytical model's accuracy by comparing the sensor model's simulated performance with its analytical counterpart.

From the table, the sensitivities of the simulated and analytical model sensors are -3.426 mV/kPa and -3.552 mV/kPa, respectively.

5. Conclusion

The mathematical modelling and simulation of the ZnO piezoelectric-based circular diaphragm-based pressure sensor for detecting 0–100 kPa are the primary objectives of this section of the research study. The simulated output data is used to validate a systematic analytical model of the sensor that is given. The proposed mathematical model can be used for further design because the simulated values are approximately equal to the calculated values.

The circular diaphragm's radius and its thickness, the thickness of the sensing material, and the voltage coefficient of the sensing material are the major components of the variables determining the sensor's output. It is discovered that in areas where tensile stress has occurred, the sensor output is negative. The output voltage for the proposed model is also seen varying linearly in magnitude but with a negative slope. It is found that the sensitivities of the analytical and simulated model sensors are -3.552 mV/kPa and -3.426 mV/kPa, respectively.

Acknowledgments

The authors extend their gratitude to the administration of Rajiv Gandhi University, Arunachal Pradesh, India, for their valuable assistance and unwavering support throughout the research project's development. It is important to note that all authors contributed equally to this study.

References

[1] Tahera Kalsoom et al., "Advances in Sensor Technologies in the Era of Smart Factory and Industry 4.0," *Sensors*, vol. 20, no. 23, pp. 1-22, 2020. [CrossRef] [Google Scholar] [Publisher Link]

[2] Kenji Uchino, "Piezoelectric Devices for Sustainability Technologies," *Reference Module in Earth Systems and Environmental Sciences*, 2022. [CrossRef] [Google Scholar] [Publisher Link]

[3] N. Soin, S.C. Anand, and T.H. Shah, *Energy Harvesting and Storage Textiles*, 2nd ed., Handbook of Technical Textiles, vol. 2, pp. 357-396, 2016. [CrossRef] [Google Scholar] [Publisher Link]

[4] Diego Galar, and Uday Kumar, *Chapter 8 - Actuators and Self-Maintenance Approaches*, eMaintenance Essential Electronic Tools for Efficiency, Academic Press, pp. 475-527, 2017. [CrossRef] [Google Scholar] [Publisher Link]

[5] Erik Schlangen et al., *Piezoelectric Energy Harvesting from Pavement*, Eco-Efficient Pavement Construction Materials, Woodhead Publishing Series in Civil and Structural Engineering, pp. 367-382, 2020. [CrossRef] [Google Scholar] [Publisher Link]

[6] Kritika Khandelwal, and Deepesh Patidar, "A Design of Optical Fiber Bragg Grating Sensor for Pressure and Temperature Monitoring," *SSRG International Journal of Electronics and Communication Engineering*, vol. 3, no. 8, pp. 6-9, 2016. [CrossRef] [Publisher Link]

[7] Amal Megdich, Mohamed Habibi, and Luc Laperrière, "A Review on 3D Printed Piezoelectric Energy Harvesters: Materials, 3D Printing Techniques, and Applications," *Materials Today Communications*, vol. 35, 2023. [CrossRef] [Google Scholar] [Publisher Link]

[8] Moirangthem Shamjit Singh, Pradip Kumar Kalita, and Maibam Sanju Meetei, "Piezoelectric-Based Square Diaphragm Pressure Sensor Modelling and Analysis Using PZT-5H and PZT-5A," *SSRG International Journal of Electrical and Electronics Engineering*, vol. 10, no. 8, pp. 1-8, 2023. [CrossRef] [Publisher Link]

[9] Vladimír Kutiš et al., "MEMS Piezoelectric Pressure Sensor-Modelling and Simulation," *Procedia Engineering*, vol. 48, pp. 338-345, 2012. [CrossRef] [Google Scholar] [Publisher Link]

[10] S. Timoshenko, and S. woinowsky-krieger, *Theory of Plates and Shells*, New York: McGraw Hill, pp. 1-580, 1959. [Google Scholar] [Publisher Link]

[11] Ansel C. Ugural, *Plates and Shells: Theory and Analysis*, 4th ed., CRC Press, pp. 1-618, 2018. [Google Scholar] [Publisher Link]

[12] Minhang Bao, *Analysis and Design Principles of MEMS Devices*, Elsevier Science, pp. 1-382, 2005. [CrossRef] [Google Scholar] [Publisher Link]

[13] Jules Fridolin Bayol, Louis Monkam, and Samuel Epesse Misse, "Analysis of the Deformation and of the Stress Intensity Factor on a Simplified Cylinder Head of a Variable Compression Rate Engine," *SSRG International Journal of Mechanical Engineering*, vol. 9, no. 3, pp. 1-14, 2022. [CrossRef] [Google Scholar] [Publisher Link]

[14] Ingo Kuehne et al., "A New Approach for MEMS Power Generation Based on a Piezoelectric Diaphragm," *Sensors and Actuators A: Physical*, vol. 142, no. 1, pp. 292-297, 2008. [CrossRef] [Google Scholar] [Publisher Link]

[15] Mario Di Giovanni, *Flat and Corrugated Diaphragm Design Handbook*, 1st ed., CRC Press, pp. 1-404, 1982. [Google Scholar] [Publisher Link]